Title: SARS-CoV-2 20I/501Y.V1 variant in the hamster model

Author list: Maxime Cochin*[1], Léa Luciani*[1], Franck Touret[1], Jean-Sélim Driouich[1], Paul-Rémi Petit[1], Grégory Moureau[1], Cécile Baronti[1], Laurence Thirion[1], Piet Maes[2], Robbert Boudewijns[3], Johan Neyts[3], Xavier de Lamballerie[1], Antoine Nougairède[1]

Affiliations:

[1] Unité des Virus Émergents (UVE: Aix-Marseille Univ-IRD 190-Inserm 1207-IHU Méditerranée Infection), Marseille, France

[2] KU Leuven Department of Microbiology, Immunology and Transplantation, Laboratory of Clinical and Epidemiological Virology, Rega Institute, Leuven, Belgium

[3] KU Leuven Department of Microbiology, Immunology and Transplantation, Laboratory of Virology and Chemotherapy, Rega Institute, Leuven, Belgium

* These authors contributed equally to this article.

Corresponding author: Antoine Nougairède (antoine.nougairede@univ-amu.fr)

Characters count: 12 641

Abstract

Late 2020, SARS-CoV-2 20I/501Y.V1 variant from lineage B.1.1.7 emerged in United Kingdom and gradually replaced the D614G strains initially involved in the global spread of the pandemic. In this study, we used a Syrian hamster model to compare a clinical strain of 20I/501Y.V1 variant with an ancestral D614G strain. The 20I/501Y.V1 variant succeeded to infect animals and to induce a pathology that mimics COVID-19. However, both strains induced replicated to almost the same level and induced a comparable disease and immune response. A slight fitness advantage was noted for the D614G strain during competition and transmission experiments. These data do not corroborate the current epidemiological situation observed in humans nor recent reports that showed a more rapid replication of the 20I/501Y.V1 variant in human reconstituted bronchial epithelium.

Text

The genetic evolution of the severe acute respiratory syndrome coronavirus 2 (SARS-CoV-2) virus is a constant concern for medical and scientific communities. From January 2020, viruses carrying the spike D614G mutation emerged in several countries (Korber et al., 2020; Volz et al., 2021; Yurkovetskiy et al., 2020). In June, D614G SARS-CoV-2 lineage B.1 became the dominant form of circulating virus worldwide and replaced the initial SARS-CoV-2 strains related to the outbreak in Wuhan, China. Experimental data from human lung epithelium and animal models revealed that the D614G substitution increased virus infectivity and transmissibility as compared to an original D614 strain (Plante et al., 2020). However, it seems that this D614G variant does not cause more severe clinical disease. In late 2020, three SARS-CoV-2 variants sharing the N501Y spike mutation located in the receptor binding motif (RBM) emerged almost simultaneously in the United Kingdom (20I/501Y.V1 variant from lineage B.1.1.7 ; initially named VOC 202012/01) (du Plessis et al., 2021), in South

Africa (501Y.V2 variant from lineage B.1.351) (CDC) and in Brazil (P.1 variant from lineage B.1.1.28.1) (Sabino et al., 2021). As previously observed with the D614G variant, the 20I/501Y.V1 variant spread rapidly and became dominant in United Kingdom in December 2020, and in many other European and non-European countries from February 2021 onwards (CoVariants.org). This similar evolution pattern seems to be associated with an improved affinity of the viral spike protein for the human angiotensin-converting enzyme 2 (ACE2) receptor (Liu et al., 2021; Zahradník et al., 2021). The 20I/501Y.V1 variant harbors 8 additional spike mutations, including substitutions and deletions, compared to D614G circulating strains. At this stage, there are few data regarding the 20I/501Y.V1 variant pathogenicity and its ability to spread more easily (Davies et al., 2021; Zhao et al., 2021). Recent studies also revealed that the active circulation of the 20I/501Y.V1 variant may not impact the risk of reinfection, the efficiency of vaccine campaigns and antibody therapies remains also unknown (Chen et al., 2021; Planas et al., 2021; Shen et al., 2021). We recently described the fitness advantage of 20I/501Y.V1 variant using a model of reconstituted bronchial human epithelium (Touret et al., 2021). In the present work, we compared the phenotype of the 20I/501Y.V1 variant (hCoV-103 19/Belgium/rega-12211513/2020 strain) with that of a D614G strain (Germany/BavPat1/2020 strain) in the Syrian hamster (*Mesocricetus auratus*) model. The study includes comparison of viral replication kinetics, transmissibility, clinical course of the disease and immunological response.

First, to detect modifications of the clinical course of the disease following infection with the 20I/501Y.V1 variant, groups of 12 three-week-old female Syrian hamsters were intranasally infected with 50µl containing $2x10^3 TCID_{50}$ of 20I/501Y.V1 or BavPat D614G strain (Figure 1.a). Follow-up of these animals until 7 days post-infection (dpi) showed with both strains a lack of weight gain compared to mock-infected group. Normalized weights (i.e. % of initial weights) of animals infected with 20I/501Y.V1 variant were significantly higher than those of

BavPat D614G group at 3, 4 and 5 dpi (p values between 0.0403 and 0.0007)(Figure 1.b). However, this difference seems to be the result of a delayed onset of disease for 20I/501Y.V1 variant since significant difference of normalized weights compared to mock-infected group began at 2 dpi for animals infected with BavPat D614G strain and at 3 dpi for those infected with the 20I/501Y.V1 variant.

Second, to further investigate viral replication, groups of 12 three-week-old female Syrian hamsters were intranasally infected with 50µl containing $2x10^3 TCID_{50}$ of each viral strain and several tissues were collected at different time points (Figure 1.a).

Viral RNA quantification was performed using a RT-qPCR assay (i) in lung and nasal wash samples collected at 2, 4 and 7 dpi, and (ii) in blood and gut samples collected at 2 and 4 dpi. Infectious titers were determined using a $TCID_{50}$ assay in lungs and nasal washes at 2 and 4 dpi. Overall, the results indicated that the 20I/501Y.V1 variant properly replicate in the hamster gut and respiratory tract. However, higher viral RNA yields were found in all samples from animals infected with BavPat D614G strain (difference ranged from 0.085 to 0.801 log_{10}). This difference was significant in lung and gut at any time point (p values ranging between 0.0332 and 0.0084) (Figure 1.c.d.e). Results of plasma did not show any significant difference (Supplemental Figure 1.a). A similar pattern was observed when assessing infectious viral loads using a $TCID_{50}$ assay (differences ranged from 0.0343 to 0.389 log_{10}) but no significant difference was found (Figure 1.f.g).

To detect more subtle differences of viral replication *in vivo*, we performed competitions experiments as previously described (Fabritus et al., 2015; Liu et al., 2021). Groups of 12 animals were simultaneously infected intranasally with 50µl containing 50% (10^3 $TCID_{50}$) of each viral strain. Lungs, nasal washes and plasma were collected at 2 and 4 dpi (Figure 1.a). Using two specific RT-qPCR systems, we estimated in all samples the proportion of each

viral genome in the viral population (expressed as BavPat D614G/20I/501Y.V1 ratios in Figure 1.h.i). Once again, results revealed that BavPat D614G strain seems to replicate a somewhat more efficiently and supplants progressively the 20I/501Y.V1 variant. Indeed, BavPat D614G/ 20I/501Y.V1 estimated ratios at 4dpi were significantly higher than those at 2 dpi in nasal washes ($p=0.0001$). Moreover, ratios at 4 dpi in nasal washes were also significantly higher than those in the infecting inoculum ($p=0.022$) (Figure 1.i). By contrast, no significant difference was found in lungs (Figure 1.h) and plasma (supplemental Figure 1.b).

To obtain a clearer picture, we compared the transmissibility of both strains in a last *in vivo* experiment. To increase the sensitivity of the procedure, groups of 12 animals were simultaneously infected intranasally with 50µl containing a low dose of each viral strain (20 $TCID_{50}$). These animals, called 'donors', firstly housed individually, were co-housed at 2 dpi with an uninfected animal, called 'contact', during a period of 6 hours in a new cage. Then, donors returned in their initial cages and were sacrificed at 3 dpi. Contact animals were sacrificed at 3 days post-contact (Figure 2.a). Using the two specific RT-qPCR systems used for competition experiments, we estimated in all samples (nasal washes and lungs) the proportion of each viral genome in the viral population (Figure 2.b). Data from lungs of donors showed for two animals, an equivalent proportion of both viruses (from 40% to 60% of each strain); for five animal, a majority (>60%) of BavPat D614G virus; and for the five remaining animals, a majority (>60%) of 20I/501Y.V1 virus. However, we did not find the same distribution in nasal washes in which we observed: for eight animals, an equivalent proportion of both viruses; for four animal, a majority of BavPat D614G virus; and for no animal, a majority of 20I/501Y.V1 virus. Consistently with this observation, we found a large majority (>75%) of BavPat D614G virus in lungs and nasal washes of eight contacts, and only two and one animals exhibited a large majority (>75%) of 20I/501Y.V1 virus in lungs and

nasal washes respectively (Figure 2.b). When analyzing the data from each pair of animals, we observed an increase of the proportion of Bavpat D614G virus between the nasal wash of the donor and lungs of the contact in almost all cases (10/12).

Altogether, our results suggest that the replication of both strains was highly comparable in hamsters. Nonetheless, using a more sensitive method, we observed that the 20I/501Y.V1 variant is outcompeted by the BavPat D614G strain; it results in an advantage for the BavPat D614G strain during transmission experiments. Notably, such results are not in line with experimental data *ex vivo* (human epithelial cultures grown at the air liquid interface) and with epidemiological observations.

We then compared transcriptional early immune signatures in lungs from animals sacrificed at 4 dpi following intranasal infection with 50µl containing $2x10^3 TCID_{50}$ of 20I/501Y.V1 or BavPat D614G strain. The expression level of seven cytokines (Interferon-γ, TNF-α, IL-6, IL-10, IL-1β, Cxcl-10, Ccl5) was quantified using RT-qPCR assays (Supplemental Figure 2; expressed as mRNA copies/γ-actin copies). Infection by both viral strains induced an important increase of CXCL10, CCL5, IFNγ, Il-6 and Il-10 expression levels ($p<0.0001$) and a moderate increase of Il-1β ($p=0.0014$ for BavPat D614G and $p=0.0281$ for 20I/501Y.V1) and TNFα ($p=0.0389$ for BavPat D614G and $p=0.0350$ for 20I/501Y.V1) expressions levels to mock-infected animals (Supplemental Figure 2). Comparison between animals infected with 20I/501Y.V1 and BavPat D614G strains did not show any significant differences of cytokines expression levels. This suggests that the early immune response induced by both viral strains is similar, in line with a recent study that did not present major differences except an upregulation of Il-6, Il-10 and IFNγ with animals infected by 20I/501Y.V1 variant (Abdelnabi et al., 2021).

Finally, we used sera collected at 7 dpi following intranasal infection with 50µl containing $2x10^3 TCID_{50}$ of 20I/501Y.V1 (n=4) or BavPat D614G (n=4) (Figure 1.a) strain to assess the level of protection against three circulating strains of SARS-CoV-2: the BavPat D614G strain, the 20I/501Y.V1 variant and a 'South-African' 20H/501Y.V2 (lineage B 1.351) variant. Sera were tested for the presence of antibodies using a 90-99% viral RNA Yield Reduction Neutralization Test (YRNT90/YRNT99) (Figure 1.j.k). Overall, results showed that animals infected with 20I/501Y.V1 or BavPat D614G strains produced similar levels of neutralization antibodies against these strains. However, all infected animals produced lower neutralization titers against the 20H/501Y.V2 variant. This difference is significant with all animals when considering YRNT90 titers (p values between 0.001 and 0.045), and significant only with animals infected with 20I/501Y.V1 variant when considering YRNT99 titers ($p < 0.048$) (Supplemental Table 1). This suggests an effective cross-immunity between 20I/501Y.V1 and BavPat D614G, but a reduced cross-protection against the 20H/501Y.V2 variant. These data indicate that only an active circulation of 20H/501Y.V2 variant might increase the risk of reinfection or failure of vaccination campaigns. This is in accordance with recently reported epidemiological observation (Graham et al., 2021; Jangra et al., 2021; Nonaka et al., 2021a, 2021b; Zucman et al., 2021).

In conclusion, our results show that the 20I/501Y.V1 variant induces a pathology that mimics human SARS-CoV-2 infection in the hamster model and can be used for preclinical analysis of vaccines and therapeutic agents. These data corroborate those of a recent study in which the same strains, a similar hamster model but higher virus inocula (10^5 $TCID_{50}$) were used (Abdelnabi et al., 2021). Since its emergence in late 2020 in Europe, the 20I/501Y.V1 variant spread across several continents and became the majority circulating strain in many countries. Moreover, data from reconstituted human airway epithelia also showed a strong replicative fitness advantage for 20I/501Y.V1 variant (Touret et al., 2021). Notably, our findings in the

hamster model are not in line with these observations. Altogether, this suggests that the hamster model may possibly not be the best model to detect weak fitness or transmissibility differences between clinical strains of SARS-CoV-2. Other animal models such as the ferret (*Mustela putorius furo*) model that is already employed to study the pathogenicity and transmissibility of other human respiratory viruses, could be valuable tools in that case. Nevertheless, in a recent study that used engineered rescued viruses derived from the USA_WA1/2020 strain, the hamster model appeared useful to detect weak fitness advantages and an increases in transmissibility of viruses that carry the N501Y and A570D spike mutations. However, the role of other mutations located in other parts of the genome of the 20I/501Y.V1 variant [more than twenty when compared to strains isolated in January-February 2020], was obviously not taken into account using this reverse genetics-based approach.

Acknowledgments

This work was supported by the European Union's Horizon 2020 Research and Innovation Programme under grant agreements no. 653316 (European Virus Archive goes global project: http://www.european-virus-archive.com/). We also thank Noémie Courtin for her technical support.

Declaration of conflicting interests

Authors declare that there is no conflict of interest

References

Abdelnabi, R., Boudewijns, R., Foo, C.S., Seldeslachts, L., Sanchez-Felipe, L., Zhang, X., Delang, L., Maes, P., Kaptein, S.J.F., Weynand, B., et al. (2021). Comparative infectivity and pathogenesis of emerging SARS-CoV-2 variants in Syrian hamsters. BioRxiv 2021.02.26.433062.

Chen, R.E., Zhang, X., Case, J.B., Winkler, E.S., Liu, Y., VanBlargan, L.A., Liu, J., Errico, J.M., Xie, X., Suryadevara, N., et al. (2021). Resistance of SARS-CoV-2 variants to neutralization by monoclonal and serum-derived polyclonal antibodies. Nat. Med. 1–10.

CDC: https://stacks.cdc.gov/view/cdc/100655

CoVariants: https://covariants.org/per-country

Davies, N.G., Jarvis, C.I., Edmunds, W.J., Jewell, N.P., Diaz-Ordaz, K., and Keogh, R.H. (2021). Increased mortality in community-tested cases of SARS-CoV-2 lineage B.1.1.7. Nature 1–5.

Fabritus, L. de, Nougairède, A., Aubry, F., Gould, E.A., and Lamballerie, X. de (2015). Attenuation of Tick-Borne Encephalitis Virus Using Large-Scale Random Codon Re-encoding. PLOS Pathog. *11*, e1004738.

Graham, M.S., Sudre, C.H., May, A., Antonelli, M., Murray, B., Varsavsky, T., Kläser, K., Canas, L.S., Molteni, E., Modat, M., et al. (2021). The effect of SARS-CoV-2 variant B.1.1.7 on symptomatology, re-infection and transmissibility. MedRxiv 2021.01.28.21250680.

Jangra, S., Ye, C., Rathnasinghe, R., Stadlbauer, D., Group, P. study, Krammer, F., Simon, V., Martinez-Sobrido, L., García-Sastre, A., and Schotsaert, M. (2021). The E484K mutation in the SARS-CoV-2 spike protein reduces but does not abolish neutralizing activity of human convalescent and post-vaccination sera. MedRxiv 2021.01.26.21250543.

Korber, B., Fischer, W.M., Gnanakaran, S., Yoon, H., Theiler, J., Abfalterer, W., Hengartner, N., Giorgi, E.E., Bhattacharya, T., Foley, B., et al. (2020). Tracking Changes in SARS-CoV-2

205 Spike: Evidence that D614G Increases Infectivity of the COVID-19 Virus. Cell *182*, 812-
206 827.e19.

207 Liu, Y., Liu, J., Plante, K.S., Plante, J.A., Xie, X., Zhang, X., Ku, Z., An, Z., Scharton, D.,
208 Schindewolf, C., et al. (2021). The N501Y spike substitution enhances SARS-CoV-2
209 transmission. BioRxiv 2021.03.08.434499.

210 Nonaka, C.K.V., Franco, M.M., Gräf, T., Mendes, A.V.A., Aguiar, R.S. de, Giovanetti, M.,
211 and Souza, B.S. de F. (2021a). Genomic Evidence of a SARS-CoV-2 Reinfection Case with
212 E484K Spike Mutation in Brazil.

213 Nonaka, C.K.V., Franco, M.M., Gräf, T., de Lorenzo Barcia, C.A., de Ávila Mendonça, R.N.,
214 de Sousa, K.A.F., Neiva, L.M.C., Fosenca, V., Mendes, A.V.A., de Aguiar, R.S., et al.
215 (2021b). Genomic Evidence of SARS-CoV-2 Reinfection Involving E484K Spike Mutation,
216 Brazil. Emerg. Infect. Dis. *27*.

217 Planas, D., Bruel, T., Grzelak, L., Guivel-Benhassine, F., Staropoli, I., Porrot, F., Planchais,
218 C., Buchrieser, J., Rajah, M.M., Bishop, E., et al. (2021). Sensitivity of infectious SARS-
219 CoV-2 B.1.1.7 and B.1.351 variants to neutralizing antibodies. Nat. Med. 1–8.

220 Plante, J.A., Liu, Y., Liu, J., Xia, H., Johnson, B.A., Lokugamage, K.G., Zhang, X., Muruato,
221 A.E., Zou, J., Fontes-Garfias, C.R., et al. (2020). Spike mutation D614G alters SARS-CoV-2
222 fitness. Nature 1–6.

223 du Plessis, L., McCrone, J.T., Zarebski, A.E., Hill, V., Ruis, C., Gutierrez, B., Raghwani, J.,
224 Ashworth, J., Colquhoun, R., Connor, T.R., et al. (2021). Establishment and lineage dynamics
225 of the SARS-CoV-2 epidemic in the UK. Science *371*, 708–712.

226 Sabino, E.C., Buss, L.F., Carvalho, M.P.S., Prete, C.A., Crispim, M.A.E., Fraiji, N.A.,
227 Pereira, R.H.M., Parag, K.V., da Silva Peixoto, P., Kraemer, M.U.G., et al. (2021).
228 Resurgence of COVID-19 in Manaus, Brazil, despite high seroprevalence. Lancet Lond. Engl.
229 *397*, 452–455.

230 Shen, X., Tang, H., McDanal, C., Wagh, K., Fischer, W., Theiler, J., Yoon, H., Li, D.,
231 Haynes, B.F., Sanders, K.O., et al. (2021). SARS-CoV-2 variant B.1.1.7 is susceptible to
232 neutralizing antibodies elicited by ancestral Spike vaccines. Cell Host Microbe *0*.

233 Touret, F., Luciani, L., Baronti, C., Cochin, M., Driouich, J.-S., Gilles, M., Thirion, L.,
234 Nougairede, A., and Lamballerie, X. de (2021). Replicative fitness SARS-CoV-2
235 20I/501Y.V1 variant in a human reconstituted bronchial epithelium. BioRxiv
236 2021.03.22.436427.

237 Volz, E., Hill, V., McCrone, J.T., Price, A., Jorgensen, D., O'Toole, Á., Southgate, J.,
238 Johnson, R., Jackson, B., Nascimento, F.F., et al. (2021). Evaluating the Effects of SARS-
239 CoV-2 Spike Mutation D614G on Transmissibility and Pathogenicity. Cell *184*, 64-75.e11.

240 Yurkovetskiy, L., Wang, X., Pascal, K.E., Tomkins-Tinch, C., Nyalile, T.P., Wang, Y., Baum,
241 A., Diehl, W.E., Dauphin, A., Carbone, C., et al. (2020). Structural and Functional Analysis
242 of the D614G SARS-CoV-2 Spike Protein Variant. Cell *183*, 739-751.e8.

Zahradník, J., Marciano, S., Shemesh, M., Zoler, E., Chiaravalli, J., Meyer, B., Rudich, Y., Dym, O., Elad, N., and Schreiber, G. (2021). SARS-CoV-2 RBD *in vitro* evolution follows contagious mutation spread, yet generates an able infection inhibitor (Biochemistry).

Zhao, S., Lou, J., Cao, L., Zheng, H., Chong, M.K.C., Chen, Z., Chan, R.W.Y., Zee, B.C.Y., Chan, P.K.S., and Wang, M.H. (2021). Quantifying the transmission advantage associated with N501Y substitution of SARS-CoV-2 in the UK: an early data-driven analysis. J. Travel Med. *28*.

Zucman, N., Uhel, F., Descamps, D., Roux, D., and Ricard, J.-D. (2021). Severe reinfection with South African SARS-CoV-2 variant 501Y.V2: A case report. Clin. Infect. Dis. Off. Publ. Infect. Dis. Soc. Am.

255 **Figures and Legends**

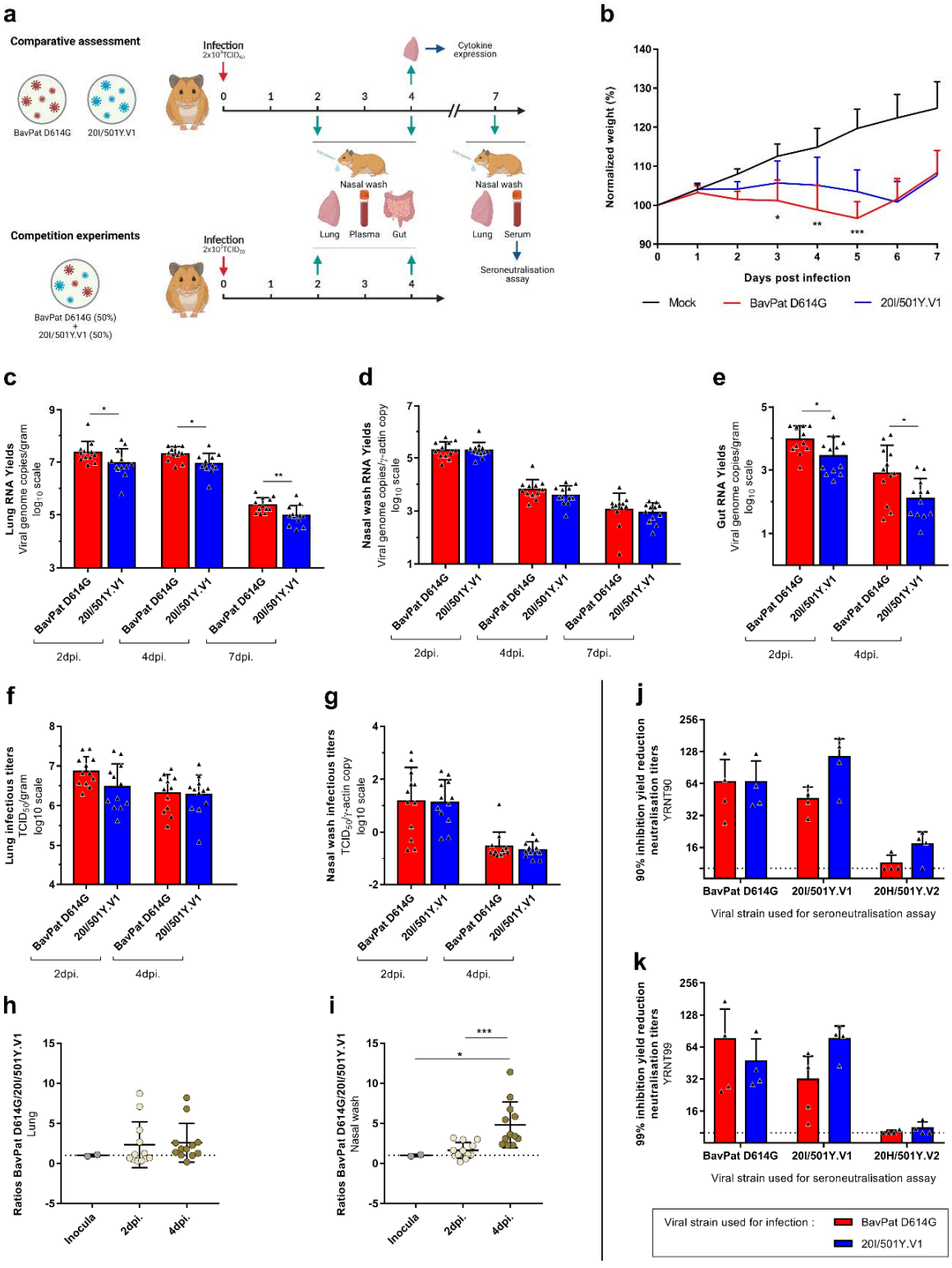

256 **Figure 1**

Figure 1: Clinical follow-up, viral replication in Syrian hamsters and seroneutralization tests. (a) Experimental timeline. Groups of 12 hamsters were intranasally infected with $2x10^3$ $TCID_{50}$ of 20I/501Y.V1 or BavPat D614G strain for comparative assessment, or with a mix (1:1) of both viral strains for competition experiment (10^3 $TCID_{50}$ of each). (b) Comparative clinical follow-up. Weights are expressed as normalized weights (i.e. % of initial weight). ***, ** and * symbols indicate that normalized weights for the 20I/501Y.V1 group are significantly higher than those of the BavPat D614G group with a p-value ranging between 0.0001-0.001, 0.001–0.01, and 0.01–0.05, respectively (Two-way ANOVA test with Tukey's post-hoc analysis). (c-e) Comparative assessment of viral RNA yields in lungs (c), nasal washes (d) and guts (e), measured using a RT-qPCR assay. ** and * symbols indicate that viral RNA yields for the 20I/501Y.V1 group are significantly lower than those of the BavPat D614G group with a p-value ranging between 0.001–0.01, and 0.01–0.05, respectively (Mann-Whitney and Unpaired t tests). (f-g) Comparative assessment of infectious titers in lungs (f) and nasal washes (g), measured using a $TCID_{50}$ assay. (h-i) Competition experiments. Two specific RT-qPCR assays were used to measure the quantity of each virus in lungs (h) and nasal washes (i). Results are expressed as [BavPat D614G/ 20I/501Y.V1] ratios. *** and * symbols indicate that ratios at 4 dpi are higher than those at 2 dpi or in inocula with a p-value ranging between 0.0001-0.001 and 0.01–0.05, respectively (Mann-Whitney tests). (j-k) Seroneutralization tests performed with sera from animals sacrificed at 7 dpi. 90% (j) and 99% (k) Yield Reduction Neutralization Titers (90-99YRNT) were determined against three strains of SAR-CoV-2: BavPat D614G, 20I/501Y.V1 and 20H/501Y.V2. Results from statistical analysis are presented in Supplemental Table 1. (b-k) Data represent mean ± SD.

279 **Figure 2**

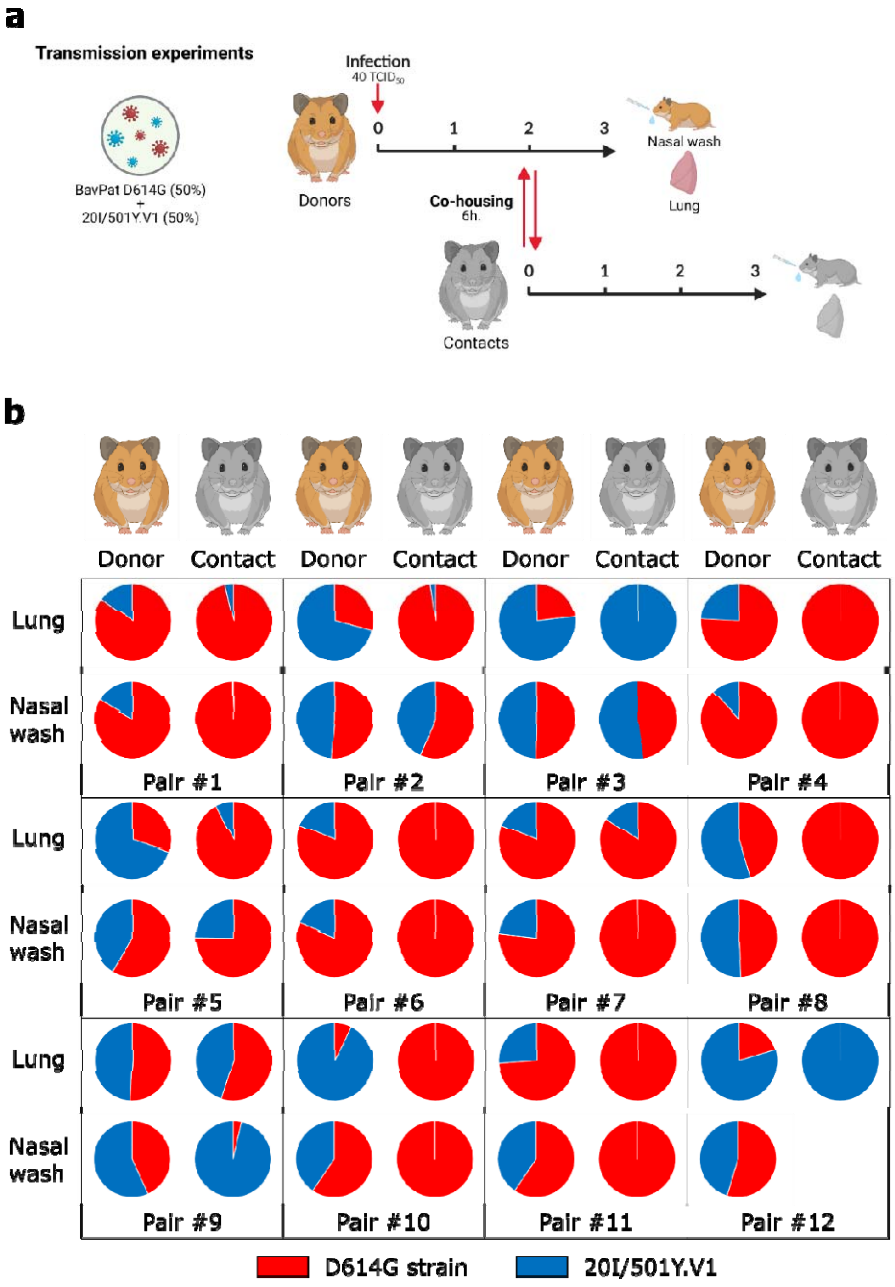

280

281 **Figure 2: Transmission experiments.** (a) Experimental timeline. A group of 12 hamsters, named
282 donors, was intranasally infected with a mix (1:1) of both viral strains for competition experiment (20
283 $TCID_{50}$ of each). At 2 dpi, each donor was co-housed with a contact animal during a period of 6 hours.
284 Donors and contacts were sacrificed at 3dpi and at 3 days post-contact respectively. (b) Graphical
285 representation of the proportion of each virus found in lungs and nasal washes for each pair of
286 animals. Two specific RT-qPCR assays were used to measure the quantity of each virus. The grey
287 circle means that no viral RNA was detected in this nasal wash.

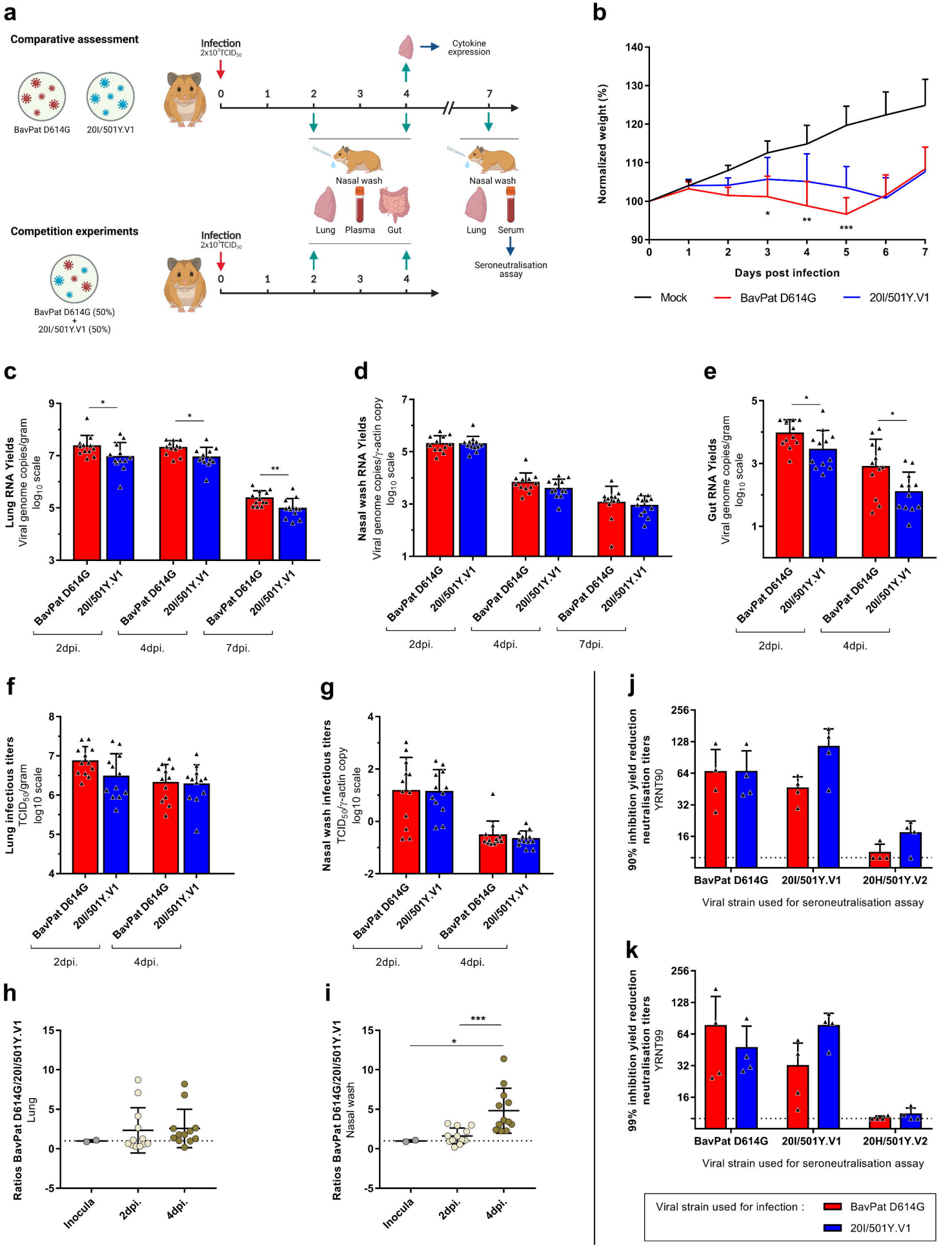
a
Comparative assessment
BavPat D614G
20I/501Y.V1
Infection
2x10⁴TCID50
Cytokine expression
Nasal wash
Lung
Plasma
Gut
Nasal wash
Lung
Serum
Seroneutralisation assay
Competition experiments
BavPat D614G (50%) + 20I/501Y.V1 (50%)
b
Normalized weight (%)
Days post infection
Mock
BavPat D614G
20I/501Y.V1
c
Lung RNA Yields
Viral genome copies/gram log10 scale
d
Nasal wash RNA Yields
Viral genome copies/r-actin copy log10 scale
e
Gut RNA Yields
Viral genome copies/gram log10 scale
2dpi.
4dpi.
7dpi.
f
Lung infectious titers
TCID50/gram log10 scale
g
Nasal wash infectious titers
TCID50/r-actin copy log10 scale
h
Ratios BavPat D614G/20I/501Y.V1
Lung
i
Ratios BavPat D614G/20I/501Y.V1
Nasal wash
Inocula
2dpi.
4dpi.
j
90% inhibition yield reduction neutralisation titers
YRNT90
BavPat D614G
20I/501Y.V1
20H/501Y.V2
Viral strain used for seroneutralisation assay
k
99% inhibition yield reduction neutralisation titers
YRNT99
Viral strain used for infection :
BavPat D614G
20I/501Y.V1

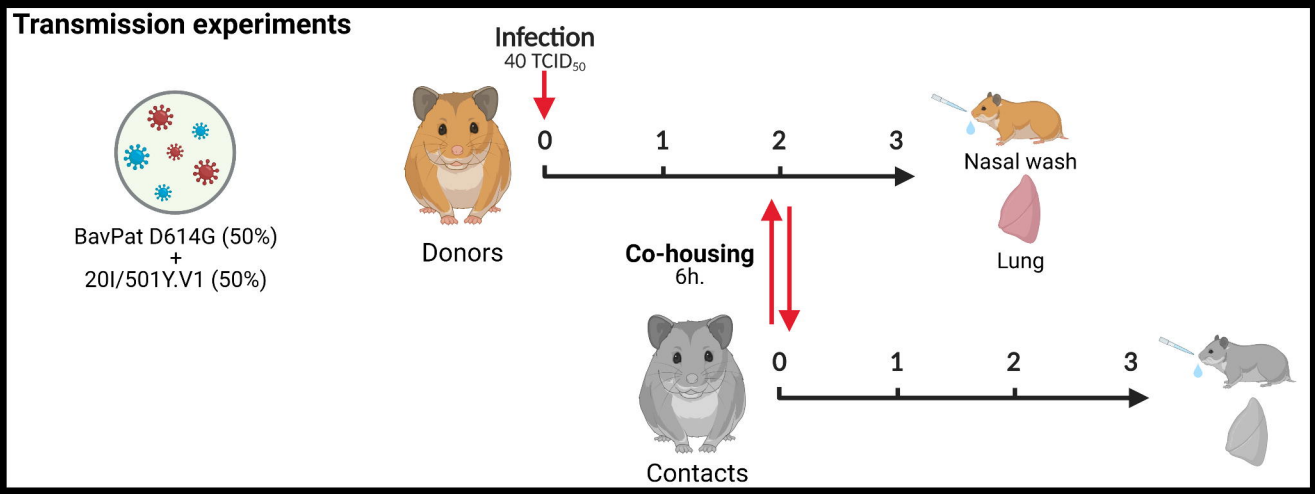
Transmission experiments
Infection
40 TCID50
BavPat D614G (50%)
+
20I/501Y.V1 (50%)
Donors
0
1
2
3
Nasal wash
Lung
Co-housing
6h.
Contacts
0
1
2
3